Int. J. Electrochem. Sci., 7 **(2012)** 10825 - 10834

International Journal of
ELECTROCHEMICAL
SCIENCE
www.electrochemsci.org

Carboxyl Multi-Wall Carbon Nanotubes Supported Pt-Ni Alloy Nanoparticles as Cathode Catalyst for Microbial Fuel Cells

Zhenhua Yan[1], *Min Wang*[1], *Baoxu Huang*[2], *Jinsheng Zhao*[1,*], *Renmin Liu*[1,*]

[1] Shandong Key Laboratory of Chemical Energy-storage and Novel Cell Technology, Liaocheng University, 252059, Liaocheng, P. R. China
[2] Department of Materials Chemistry, Liaocheng University, 252059, Liaocheng, P. R. China
[*]E-mail: j.s.zhao@163.com; liurenmin@126.com

Received: 9 September 2012 / *Accepted:* 16 October 2012 / *Published:* 1 November 2012

This work discusses a low-cost and high performance catalyst of the oxygen reduction reaction (ORR) in microbial fuel cells (MFCs). The catalyst was formed by Pt–Ni (15 wt% Pt) nanoparticles dispersed on carboxyl multi-wall carbon nanotubes (Pt-Ni/MWNT). The catalyst particle presents a nano-crystalline structure and has an average diameter of ca.7.1 nm based on the X-ray diffraction and transmission electron microscopy measurement. The electrocatalytic stability and activity of the catalyst was evaluated by cyclic voltammogram and chronopotentiometry. The MFC with a Pt-Ni/MWNT cathode produced a maximum power density of 1.22 W/m^2, which was close to that with a Pt/C (20 wt% Pt) cathode (1.40 W/m^2); the Coulombic efficiency reaches 31.6%, which was better than that of the Pt/C (29.3%). The total cost of a Pt-Ni/MWNT catalyst was much lower than that of a Pt/C catalyst. Thus, the Pt-Ni/MWNT probably provides a new solution for finding effective cathode materials for MFC.

Keywords: Microbial full cell; Oxygen reduction reaction; Catalyst; Pt-Ni/MWNT

1. INTRODUCTION

The microbial fuel cell technology has drawn increasing attention in using wastewater as the anodic “fuel” to generate electricity and accomplish pollutant treatment simultaneously [1-4]. It provides an alternative method for simultaneous energy production and wastewater treatment. In a MFC, consumption of organic compounds by microorganisms at the anode is accompanied by electron transfer to the anode and proton release. The protons flow through the electrolyte and the electrons flow through the external circuit to reach the cathode, where they are used along with electrons to accomplish oxygen reduction to water [5, 6]. The MFC technology is promising; however, several limiting factors may weigh heavily against the magnitude of power yield before it obtains a significant

share of the energy market. Owing to slow kinetics of cathode ORR in pH-neutral aqueous electrolyte, power density generated from a MFC is commonly controlled by the cathode performance [7-10]. The biggest technical challenge in MFC is the poor kinetics of the cathodic reaction and the high costs of Pt-based electrocatalysts， even on the most active Pt surface, the over-potential of ORR is considerable [8].

Pt is the most active oxygen reduction electrocatalyst, but the high cost and sensitivity to poisoning of Pt electrocatalysts brings about serious challenges for MFC technology commercialization [12-14]. So far, most efforts have focused on the development of low-cost, stable and more active electrocatalysts to replace Pt. A variety of chemical catalysts have been studied for ORR, mainly including platinum-based alloy Pt–M (M=Co, Fe, Cu, Pd and Ni etc.) [12-20], metal-N4 macrocycles like porphyrines, phthalocyanines, MnO_2 [21-26], and carbon powders [27]. Although recent technological improvements have reduced the amount of Pt required, neither the fabrication process of catalyst is rigorous nor the market-price limitations for mass production have not yet been satisfied. It's especially compelling for synthesize out high active, stable and low-cost electrocatalysts for ORR.

High surface area electrocatalyst support materials are essential to disperse electrocatalyst nanoparticles uniformly to reduce the electrocatalyst loading and aid in improving the MFC performance [28]. In this regard, carboxyl multi-wall carbon nanotubes (MWNTs) appear to be an ideal candidate as an electrocatalyst support material due to their large surface area, good thermal and chemical stability, as well as high electrical conductivity [29-30]. Most of previous studies are use carbon black as support material, the report about the synthesis of carboxyl multi-wall carbon nanotubes-supported Pt/Ni catalyst for MFC is scanty. So the primary objective of this study was to prepare highly stable and active ORR catalysts for MFC by supporting Pt-Ni catalysts on MWNTs (be referred to as Pt-Ni/MWNT) through a comparatively mild method.

In this work we have used $NaBH_4$ as reducing agent and OH^- ions as stabilizing agent to deposit Pt-Ni nanoparticles on MWNTs, although these Pt-Ni/MWNT (atomic ratio, Pt: Ni = 1:1,15 wt% Pt) alloy catalysts contain half reduced content of Pt, they exhibit about the same catalytic activity towards oxygen reduction compared to pure platinum catalyst. Cyclic voltammetry (CV) measurement was used to study the electrocatalytic stability. X-ray diffraction (XRD) and transmission electron microscopy (TEM) measurements were employed to observe the catalyst characterization. We also investigated its performance in an air cathode single chamber MFC. For comparison, a commercially available oxygen reduction electrocatalyst of 20 wt% Pt/C was also tested.

2. EXPERIMENTAL

2.1 Electrocatalyst preparation

Pt-Ni/MWNT catalyst (15 wt% Pt) was reduced by a well-known ultrasonic synthesis method, using $NaBH_4$ (Aladdin) as reducing agent. The typical preparation procedure was as follow: The appropriate amounts of COOH-CNT (Timesnano) were dissolved in deionized water with vigorous ultrasonically stirring for 20 min. A mixture of N_i $(NO_3)_2 \cdot 6H_2O$ (Aladdin) and $H_2PtCl_6 \cdot 6H_2O$

(Aladdin) was dissolved in deionized water with the Pt: Ni (atomic ratio) =1:1, and then this mixture was dropwise added to the above ink with vigorous electromagnetic stirring. After stirring for 24 h, the pH of the entire solution was adjusted to 12 by adding NaOH, the reducing agent solution $NaBH_4$ were slowly added to the above solution and keep stirring for 8 h, followed by filtering, washing, and drying at 60 ºC.

2.2 Electrode preparation

Carbon cloths (3×5 cm) (non-wet proofed, type A, E-TEK) were used as anodes. All the carbon cloths were first cleaned by soaking them in pure acetone (Aladdin) overnight, then acid treated by soaking the cloths in a solution of ammonium peroxydisulfate (200 g/L) and concentrated sulfuric acid (100 mL/L) for 15 min. After that, carbon cloths were heat-treated in a muffle furnace at 450 ºC for 30 min. Following treatments, all cloths were washed three times with distilled water before being used in MFCs [31]. Cathodes were also made of carbon cloth with a projected surface area of 4.5 cm^2; the water proof layer was made as described by previous report [22, 33]: Coated with one layer of a mixture of Vulcan XC-72 (2.5 mg/cm^2) and poly tetrafluoroethylene (PTFE, 60%), and three layers of PTFE (30%) on the air-facing side. The catalytic layer was then prepared as follows: 30 mg Pt-Ni/MWNT catalyst (with a Pt loading of 0.375 mg/cm^2), 200 μL of 5 wt% Nafion solution and 100 μL pure iso-propanol were blended in a plastic sample vial, the suspension was coated onto the surface of a carbon cloth. For comparison, cathodes with Pt/C (20 wt%, with a Pt loading of 0.5 mg/cm^2) were prepared using the same method. All electrodes were dried at room temperature for at least 24 h before use.

2.3 MFC construction and operation

Air-cathode single chamber cylindrical MFCs (length 6 cm, diameter 2.4 cm, volume 27 mL) were constructed, and wired to an external resistor (1000 Ω). The cathode was placed on one side of MFC with the oxygen catalyst coating layer facing to the anode, with the PTFE layer exposed directly to air. The anode was positioned (perpendicularly to the cathode) in the other side of chamber, with a distance of 1.0 cm from the cathode and no membrane between the two electrodes. MFC reactors were inoculated using pre-domesticated bacteria from another double chamber MFC. MFCs were inoculated using solution containing glucose (1 g/L) and a phosphate buffered nutrient medium (PBM) containing NH_4Cl (0.31 g/L), $NaH_2PO_4 \cdot H_2O$ (4.97 g/L), $Na_2HPO_4 \cdot H_2O$ (2.75 g/L), KCl (0.13 g/L), and a metal (12.5 mL) and vitamin (12.5 mL) solution [21, 33]. The solution was replaced at the end of each fed-batch cycle, defined as a voltage less than 50 mV. All tests were conducted in a 30 ºC temperature, and were carried out in two parallel samples.

2.4 Analysis and calculation

X-ray diffraction (XRD; D-MAX 2200VPC, RIGAKU) was performed to characterize the catalyst by using Cu Ka radiation. Data acquisition was carried out in the scanning angle range of 20-

90°. In order to estimate the particle size from XRD, Scherrer equation was used [34]. For this purpose, the (2 2 0) peak of the Pt around 2-thea=68° was selected. All X-ray diffraction patterns were analyzed using Jade 6.0 software. TEM measurements were carried out on a JEOL-2010; the acceleration voltage was 200 kV. The TEM data were analyzed by Digital Micrograph Demo.

In order to investigate the ORR characterization of various catalysts, cyclic voltammogram (CV) were performed using an electrochemical work station (CHI 760) with the conventional three-electrode system. A saturated calomel electrode (SCE) and a Pt wire were used as the reference and counter electrode, respectively. The catalysts coated glassy carbon (GC, 3.0 mm diameter) electrodes were used as working electrodes. Homogeneous catalyst ink is prepared by dispersing 10 mg catalyst in 0.25 mL 5 wt.% Nafion solution and 1.25 mL ultrapure water by sonicating for 30 min, and 3.0 μl of the slurry was deposited on the glassy carbon electrode (area 0.07065 cm^2), then dried at room temperature. After fabrication, the electrodes are immersed in O_2-saturated 0.5 M H_2SO_4 and voltammograms are recorded. All the potential values are given with respect to SCE in the report.

Cathode potentials were measured in PBM in the absence of microorganisms by chronopotentiometry using an electrochemical work station (CHI 760), using a three-chambered electrochemical cell containing a working electrode (cathode electrode with 0.64 cm^2 projected surface area), a counter electrode (platinum plate with a projected surface area of 2 cm^2), and a SCE reference electrode. The catalyst-coated side of the cathode was placed facing the solution, with the uncoated side exposed directly to air. The potential for each current was obtained by applying a constant current for 60 min. A curve of the cathode potentials against current densities was used to evaluate the performance of cathodes. For fixed current density, the higher the potential the better the performance of the cathode material.

The polarization curves and the power density curves were obtained by varying the external resistance (R) from 20000 to 20 Ω, when the voltage output was in steady-state after keep 20000 Ω for an hour, and the voltage (V) changing with the external resistance in the MFC was recorded by a data acquisition system connected to a computer every 10 min. At each resistance (R), MFCs were operated for two batches to ensure repeatable voltage output. The power density (P, mW/m^2) was calculated by the equation 1.

$$P = \frac{V_{cell}^2}{R_{ex} A} \quad (1)$$

and the current density was calculated by equation 2.

$$I = \frac{V_{cell}}{R_{ex} A} \quad (2)$$

in which A is the project area of the cathode. Internal resistance (R_i) was calculated by linear regression of voltage *vs.* current and open circuit voltage U_{OCV} was the voltage obtained at zero current. The Coulombic efficiency (CE) was calculated from the total current production (Q_{ex}) and the total initial added COD of glucose (equation 3). The chemistry oxygen demand of glucose is 1.063 g/L.

$$CE = \frac{Q_{ex}}{COD_{glucose} \times V \times F \times b \div M} \quad (3)$$

in which V is liquid volume (0.02 L), F is Faraday's constant (96485 C/mol of e^-) and b is mol of e^- produced per mol of O_2 (4 mol/mol), M is the mole mass of O_2 (32 g/mol).

3. RESULTS AND DISCUSSION

Fig. 1 shows the X-ray diffraction patterns for the Pt-Ni/MWNT nanoparticles, a commercial Pt/C catalyst and unmodified Vulcan XC-72 carbon powder. The broad peak at 2-thea approximately 25º is characteristic of the carbon. The XRD pattern for catalysts is very similar to that for Pt/C, without any obvious additional peaks, indicating that the electrocatalysts present the face centered cubic (fcc) structure of platinum. According to previous reports [35-37] the lack of extra peaks indicates that the Pt-Ni/MWNT alloys have disordered structures with Ni atoms distributed randomly at the Pt positions. The reflection peaks of the Pt-Ni/MWNT samples are shifted to higher angles compared to those of Pt/C, indicating a contraction of the unit cell lattice arising from substituting the larger Pt atoms for the smaller Ni and alloy formation between metallic phases. The Pt/C and Pt-Ni/MWNT catalyst particle sizes, calculated from XRD data (2 2 0) peak of the Pt use the Scherrer equation by Jade software, are 3.8 and 6.8 nm, respectively.

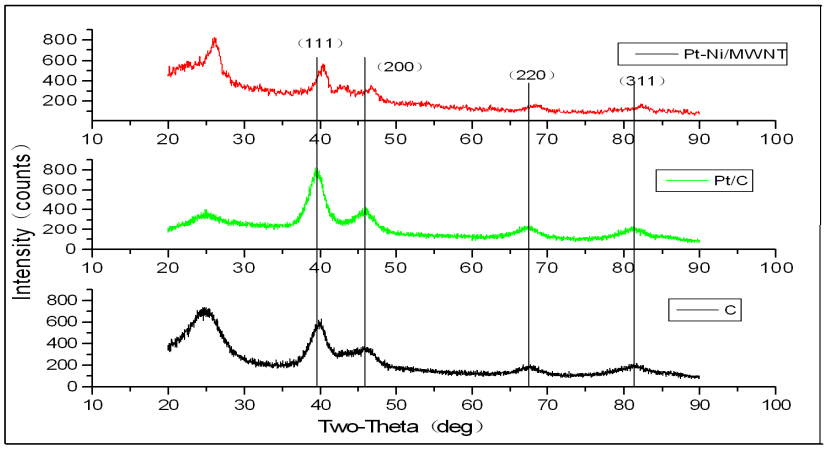

Figure 1. X-ray diffraction patterns for the Pt-Ni/MWNT, commercial Pt/C 20% catalyst and unmodified Vulcan XC-72 carbon powder

Fig. 2 presents TEM images and histograms of the Pt-Ni/MWNT catalysts. As can be observed from the TEM micrograph, the Pt-Ni particles appears as small particles, which were well and homogeneously dispersed on the multi-wall carbon nanotubes. The mean particle size was 7.4 nm, which was calculated according to equation 4.

$$d = \frac{\sum_i n_i d_i}{\sum_i n_i} \quad (4)$$

where n_i is the frequency of occurrence of particles with size d_i. Average particle size of 7.4 nm was obtained for Pt-Ni/MWNT catalysts. The average particle size of Pt-Ni/MWNT catalyst calculated from the TEM image is in good agreement with this measured by the Scherrer equation in the XRD peak.

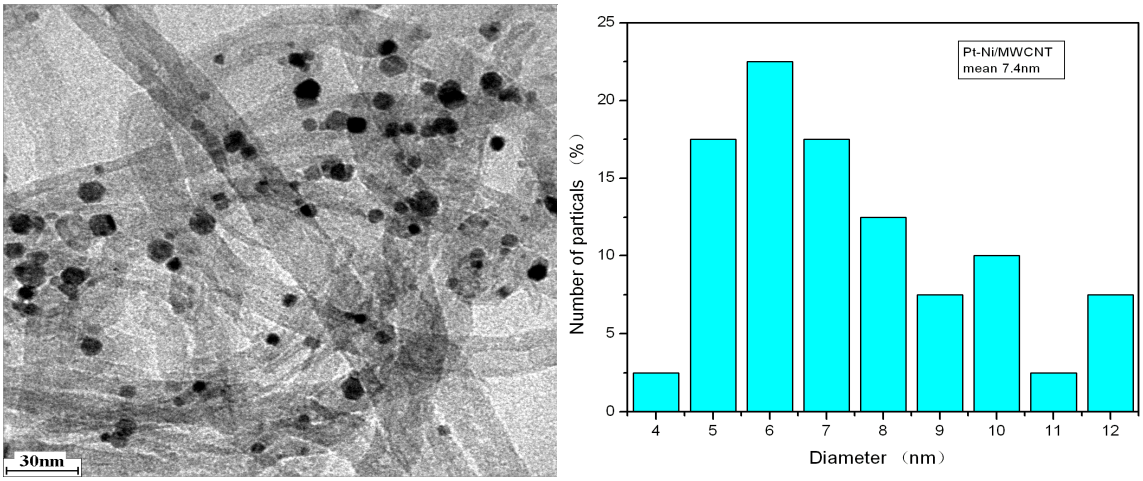

Figure 2. TEM images and histogram of the Pt-Ni/MWNT catalysts

The electrochemical performance of catalyst materials is very sensitive to their surface composition and structures. Therefore electrocatalytic activity towards ORR of the as-prepared Pt-Ni/MWNT nanoparticles was evaluated by cyclic voltammetry (CV). The measurements were performed in a 0.5 M H_2SO_4 aqueous electrolyte. Fig. 3 shows the cyclic voltammograms of Pt-Ni/MWNT catalysts with different scan rates (from 20 to 180 mV/s). A linearity of the cathodic or anodic peak currents with scan rates demonstrated that the redox reaction of Pt-Ni was a diffusionless surface-controlled process, confirming that the immobilized Pt-Ni/MWNT was rather stable. The hydrogen adsorption/desorption peak and the preoxidation/reduction peak for the electrocatalysts was clearly obtained at -0.19 V.

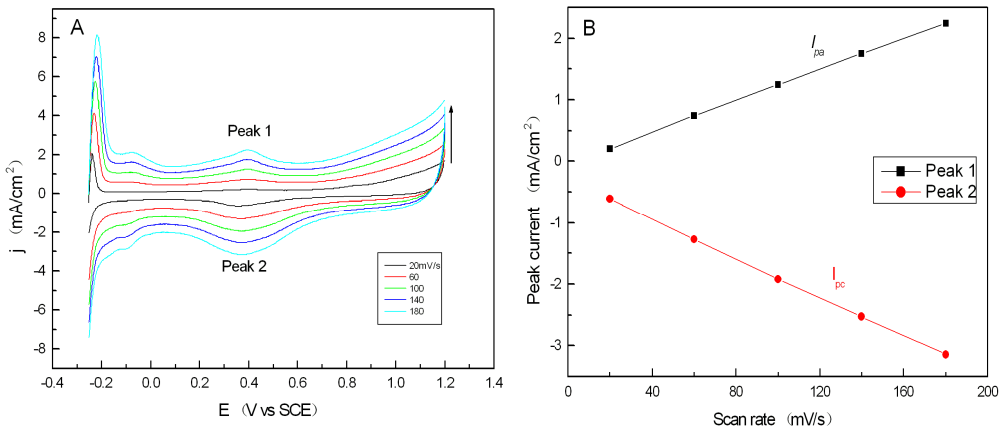

Figure 3. CVs of Pt-Ni/MWNT catalysts with different scan rates (A) and the peak currents as a linear function of scan rates (B). The peak 1–2 was in accordance with the marks in graph A.

The performance of a Pt-Ni/MWNT cathode was compared to Pt/C catalyst cathode using chronopotentiometry as shown in Fig 4. The potential decreased rapidly at current densities less than 0.4 mA/cm^2. The open circuit potential (OCP) of the Pt-Ni/MWNT and Pt/C catalyst cathode is 280 mV and 300 mV (vs SCE) respectively. Though these Pt-Ni/MWNT alloy catalysts contain quarter content of Pt less than Pt/C, the potentials produced by the commercially available Pt/C catalyst cathode were only a little higher (20-28.5 mV) than those obtained using the Pt-Ni/MWNT catalyst cathode.

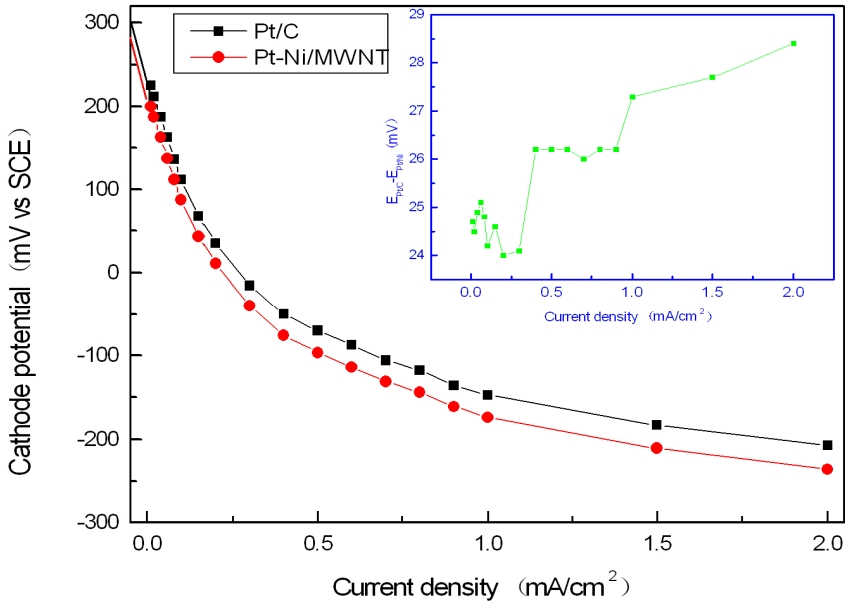

Figure 4. Comparison of cathode potential measured in the electrochemical cell for the cathodes with Pt/C and Pt-Ni/MWNT catalysts

In order to evaluate the catalytic active and long-term stability of the catalyst, the cell voltage over a whole operation period were examined in single-chamber MFCs. Electricity generation with 1g/L glucose for Pt/C and Pt-Ni/MWNT alloy catalysts was compared in the MFCs (Fig 5A). The maximal output voltage of MFC with the Pt-Ni/MWNT ally catalyst is comparable with Pt/C catalysts, only 10-20 mV lower than the MFC with Pt/C catalyst, and the maximum voltage of each cycle was stable at around 0.57 V and 0.585 V respectively. As is shown in the Fig 5A, all circles of the MFC with Pt-Ni/MWNT ally catalyst can reach maximum voltage within 6 hours, but Pt/C catalyst need 10 hours at least, and the former's electricity generation circle (80-100 hours) is shorter than the latter's (105-130 hours). In addition, the Coulombic efficiency was higher with Pt-Ni/MWNT ally catalyst (31.6%) than Pt/C catalyst (29.3%), which was calculated from the first circle (Fig 5B). Thereby we could conclude that the performance of Pt-Ni/MWNT ally catalyst in the MFC is about the same than Pt/C catalyst.

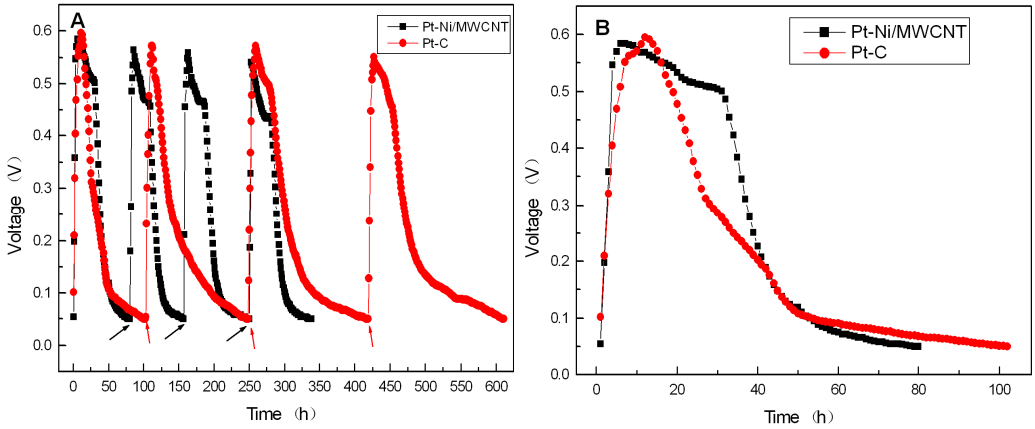

Figure 5. Comparison voltage generations for Pt/C and Pt-Ni/MWNT alloy catalysts across a 1000Ω external resistance in air cathode single-chamber MFCs over the long-term operation（A）, the concentration for each substrate was 1 g/L glucose. The arrows indicate the substrate addition. Voltage generations for the first circle (B).

To evaluate the efficiency of different catalysts, the performances of MFCs with Pt-Ni/MWNT and Pt/C cathodes were monitored. The obtained power densities and polarization curves are shown in Fig. 6. The maximum power density of the MFC with a Pt-Ni/MWNT cathode was 1.22 ±0.016 W/m^2, which was a little lower than that with a Pt/C cathode (1.405 ± 0.014 W/m^2). Polarization was conducted by changing the external circuit load, once stabilized performance of MFC was observed. There was a sudden drop of cell voltage at relatively higher current and lower external resistance (20–100 Ω) in all polarization tests. Internal resistance was estimated from the slope of the plot of voltage versus current, and it was observed to be 73 Ω and 71 Ω in Pt-Ni/MWNT cathode and Pt/C cathode MFCs, respectively. The electrochemical reaction rates could be evaluated by the open circuit potential (OCP). A higher OCP value was related to a higher reaction rate [6]. The OCP of the MFC with a Pt-

Ni/MWNT cathode was 0.74 ±0.01 V, which was similar to that with a Pt/C cathode (0.76 ±0.01 V), indicating the ORR rate of the Pt-Ni/MWNT catalyst compare with the Pt/C catalyst.

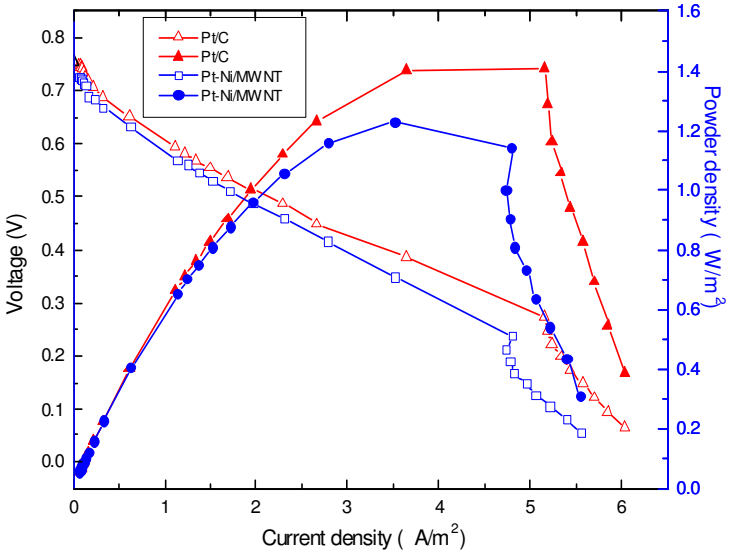

Figure 6. Power density curve and polarization curve for Pt-Ni/MWNT ally catalyst (Pt: Ni atomic ratio of 1:1; 0.375 mg Pt/cm^2), and Pt/C (0.5 mg Pt/cm^2).

4. CONCLUSIONS

The Pt-Ni/MWNT alloy nanoparticles were investigated as replacement for commercial Pt/C as the cathode catalyst in MFCs in this study. Studies with TEM and XRD reveal that Pt-Ni/MWNT nanoparticles are approximately 7.4 nm. The electrochemical results demonstrate that the catalytic of the Pt-Ni/MWNT was stable and possess highly ORR catalyze active. The power output of the MFC with a Pt-Ni/MWNT cathode was much close to that with a Pt/C cathode, while, the price of a Pt-Ni/MWNT catalyst was approximately three-quarter of Pt/C catalyst. In terms of easy fabrication, lower cost and high power production, Pt-Ni/MWNT showed a great potential to be used as a cost-effective catalyst in air cathode MFCs.

ACKNOWLEDGEMENTS
The work was financially support by the National Natural Science Foundation of China (20906043, 31170110), the Promotive research fund for young and middle-aged scientists of Shandong Province (2009BSB01453), the Natural Science Foundation of Shandong province (ZR2010BQ009, , ZR2011EL002) and the Taishan Scholarship of Shandong Province.

References

1. K. Rabaey, W. Verstraete, *Trends. Biotechnol*, 23 (2005) 291–298

2. B. Logan, J.M. Regan, *Environ. Sci. Technol*, 40 (2006) 5172–5180
3. D.R. Lovely, *Curr. Opin. Biotech,* 17 (2006) 327–332
4. Y. Li, A.H. Lu, H.R. Ding, X. Wang, C.Q. Wang, C.P. Zeng, Y.H. Yan, *Electrochem. Commun,* 12 (2010) 944-947
5. B.E. Logan, B. Hamelers, R. Rozendal, U. Schroder, J. Keller, S. Freguia, P. Aelterman, W. Verstraete, K. Rabaey, *Environ. Sci. Technol,* 40 (2006) 5181
6. D.R. Lovley, *Curr. Opin. Biotech,* 19 (2008) 564
7. G.C. Gil, I.S. Chang, B.H. Kim, M. Kim, J.K. Jang, H.S. Park, H.J. Kim, *Biosens. Bioelectron,* 18 (2003) 327
8. J. K. Nørskov, J. Rossmeisl, A. Logadottir, and L. Lindqvist, J. Phys. Chem. B 108 (2004) 17886 - 17892
9. H. Rismani-Yazdi, S.M. Carver, A.D. Christy, O.H. Tuovinen, *J. Power. Sources,* 180 (2008) 683
10. A. Sarkar, A.V. Murugan, A. Manthiram, *J. Phys. Chem. C,* 112 (2008) 1203
11. J.N. Zhang, S.J. You, Y.X. Yuan, Q.L. Zhao, G.D. Zhang, *Electrochem. Commun,* 13 (2011) 903–905
12. J.L. Fermandez, D.A. Walsh, A.J. Bard, *J. Am. Chem. Soc,* 127 (2005) 35
13. A. Sarkar, A.V. Murugan, A. Manthiram, *J. Phys. Chem. C,* 112 (2008) 12037
14. R.F. Wang, H. Li, S. Ji, H. Wang, Z.Q. Lei, *Electrochim. Acta,* 55 (2010) 1519–1522
15. J. Ricardo, C. Salgado, E. Antolini, E.R. Gonzalez. *Appl. Catal. B-Environ* 57 (2005) 283–290
16. S.J Guo, S. Sun, *J. Am. Chem. Soc,* 134 (2012) 2492–2495
17. Q.H. Huang, H Yang, Y.W Tang, T.H. Lu, D. L. Akins. *Electrochem. Commun,* 8 (2006) 1220–1224
18. T. Lopes, E. Antolini, E.R. Gonzalez, *Int. J. Hydrogen. Energ,* 33 (2008) 5563 – 5570
19. K.C. Neyerlin, R. Srivastava, C.F. Yu, P. Strasser, *J. Power. Sources,* 186 (2009) 261–267
20. H.M. Wu, D. Wexler, G.X. Wang. *J. Alloy. Compd,* 488 (2009) 195–198
21. Y. Yuan, S. Zhou, L. Zhuang, *J. Power Sources,* 195 (2010) 3490
22. J.R. Kim, J.Y . Kim, S.B. Han, K.W. Park, G.D. Saratale, S.E. Oh, *Bioresource. Technol,* 102 (2011) 342–347
23. S.A. Cheng, H. Liu, B.E. Logan, *Environ. Sci. Technol*, 40 (2006) 364-369
24. F. Zhao, F. Harnisch, U. Schröder, F. Scholz, P. Bogdanoff, I. Herrmann, *Electrochem. Commun,* 7 (2005) 1405
25. X. Li, B.X. Hu, S. Suib, Y. Lei, B.K. Li, *J. Power. Sources,* 195 (2010) 2586
26. L. Zhang, C. Liu, L. Zhuang, W. Li, S. Zhou, J. Zhang, *Biosens. Bioelectron*, 24 (2009) 2825
27. B. Erable, N. Duteanu, S.M. Senthil Kumar, Y.J. Feng, M.M. Ghangrekar, K. Scott, *Electrochem. Commun,* 11 (2009) 1547
28. B.P. Vinayan, R. I. Jafri, R. Nagar, N. Rajalakshmi, K. Sethupathi, S. Ramaprabhu, *Int. J. Hydrogen. Energ,* 37 (2011) 412-421
29. R. I. Jafri, S. Ramaprabhu, *Int. J. Hydrogen. Energy,* 35(2010)1339-1346.
30. N. Jha, A.L.M. Reddy, M.M. Shaijumon, N. Rajalakshmi, S. Ramaprabhu, *Int. J. Hydrogen. Energy,* 2008;33:427-433
31. Y.J. Feng, Q. Yang, X. Wang, B. E. Logan, *J. Power. Sources,* 195 (2010) 1841–1844
32. T. Catal, D. Cysneiros, V. O'Flaherty, D. Leech, *Bioresource. Technol,* 102 (2011) 404–410
33. D. R. Lovley, E. J. Phillips, *Appl. Environ. Microb,* 54 (1988) 1472-1480
34. B.E. Warren, *X-ray Diffraction*, Addison-Wesley, Reading, MA, (1969)
35. L.Xiong, A. Manthiram, *J. Electrochem. Soc*, 152 (2005) 697
36. L.G.R.A. Santos, C.H.F. Oliveira, I.R. Moraes, E.A. Ticianelli, *J. Electroanal. Chem,* 596 (2006) 141–148
37. Y.W. Lee, S.E. Oh, K.W. Park, *Electrochem. Commun,* 13 (2011) 1300-1303